Protoplasma (1992) 166: 89–98

PROTOPLASMA

Specialized calciferous cells in the marine alga *Rhodogorgon carriebowensis* and their implications for models of red algal calcification

C. M. Pueschel*, H. H. Eichelberger, and **H. N. Trick**

Department of Biological Sciences, State University of New York at Binghamton, Binghamton, New York

Received January 22, 1991
Accepted April 30, 1991

Summary. Calcification in *Rhodogorgon carriebowensis* J. Norris et Bucher was associated with a particular cell type in the cortex. Calciferous cells were 4–6 times the length of cortical assimilatory cells. The distal two-thirds of the calcifying cell was invested with a thick wall that stained with periodic acid Schiff. Thick fibrils formed a reticulum and surrounded grains of calcium carbonate that ranged in shape from rhombohedral to subspherical and were up to 200 nm in greatest dimension. The proximal third of the cell was a tapering uncalcified stalk. The narrow base of the cell was attached to the subtending cell of the fascicle by a normal septum with a pit plug. The cell within the calcified wall matrix was usually flattened and had a very small volume. Cellular contents were dense; even when organelles could be discerned, they could not be identified. X-ray microanalysis revealed that other elements commonly found mixed with calcium carbonate are virtually absent from mineral deposits in *R. carriebowensis*, but electron diffraction study showed d-spacings that varied from those of pure calcite. Current models of red algal calcification are discussed in light of the findings on this alga.

Keywords: Calcification; Calcium carbonate; *Rhodogorgon*; Red algae.

Abbreviations: $CaCO_3$ calcium carbonate; DIC differential interference contrast; PAS periodic acid Schiff; SEM scanning electron microscopy; TEM transmission electron microscopy.

Introduction

Calcium carbonate mineralization is a widespread phenomenon in the algae. An entire order of red algae, the Corallinales, is characterized by the deposition of calcite. Their cell walls are impregnated with $CaCO_3$ in such abundance that for many years the algal nature of the group was unclear (Silva and Johansen 1986). Particular members of other red algal orders, especially the Nemaliales, calcify less extensively, and they deposit aragonite rather than calcite (Borowitzka et al. 1974). Norris and Bucher (1989) reported that both species of the newly described red alga, *Rhodogorgon*, deposit $CaCO_3$ in association with specialized cells and that the mineral form is calcite. *Rhodogorgon* appears to have affinities with the Batrachospermales (Norris and Bucher 1989, Pueschel et al. 1992), an otherwise exclusively freshwater order. It is the first marine non-corallinalean red alga found to have calcite and the first red alga reported to have specialized calcified cells.

The general ultrastructure of *Rhodogorgon carriebowensis* J. Norris et Bucher was described by Pueschel et al. (1992). The present study focuses on the unique calciferous cells. Calcium carbonate deposits and features of these specialized cells involved in calcification are described based on light microscopy and scanning and transmission electron microscopy. Analysis of the mineral deposits using X-ray microanalysis and electron diffraction is reported. Implications of this study for models of red algal calcification are considered.

Materials and methods

Collection data and preparatory procedures for light and electron microscopy of *Rhodogorgon carriebowensis* are described in Pueschel et al. (1992). To obtain internal views of the mineralized cells walls of calciferous cells, specimens were cryofractured in liquid nitrogen at the 75% ethanol stage of dehydration. Some specimens were exposed to 0.1 N HCl in 75% ethanol for 10 min during the dehydration series to remove calcification. Dehydrated specimens were dried by the critical point method or were air dried after replacement of ethanol dehydrant by two changes of 1,1,1,3,3-hexamethyldisilazane (Nation 1983). Sections prepared for TEM examination of

* Correspondence and reprints: Department of Biological Sciences, State University of New York at Binghamton, Binghamton, NY 13902-6000, U.S.A.

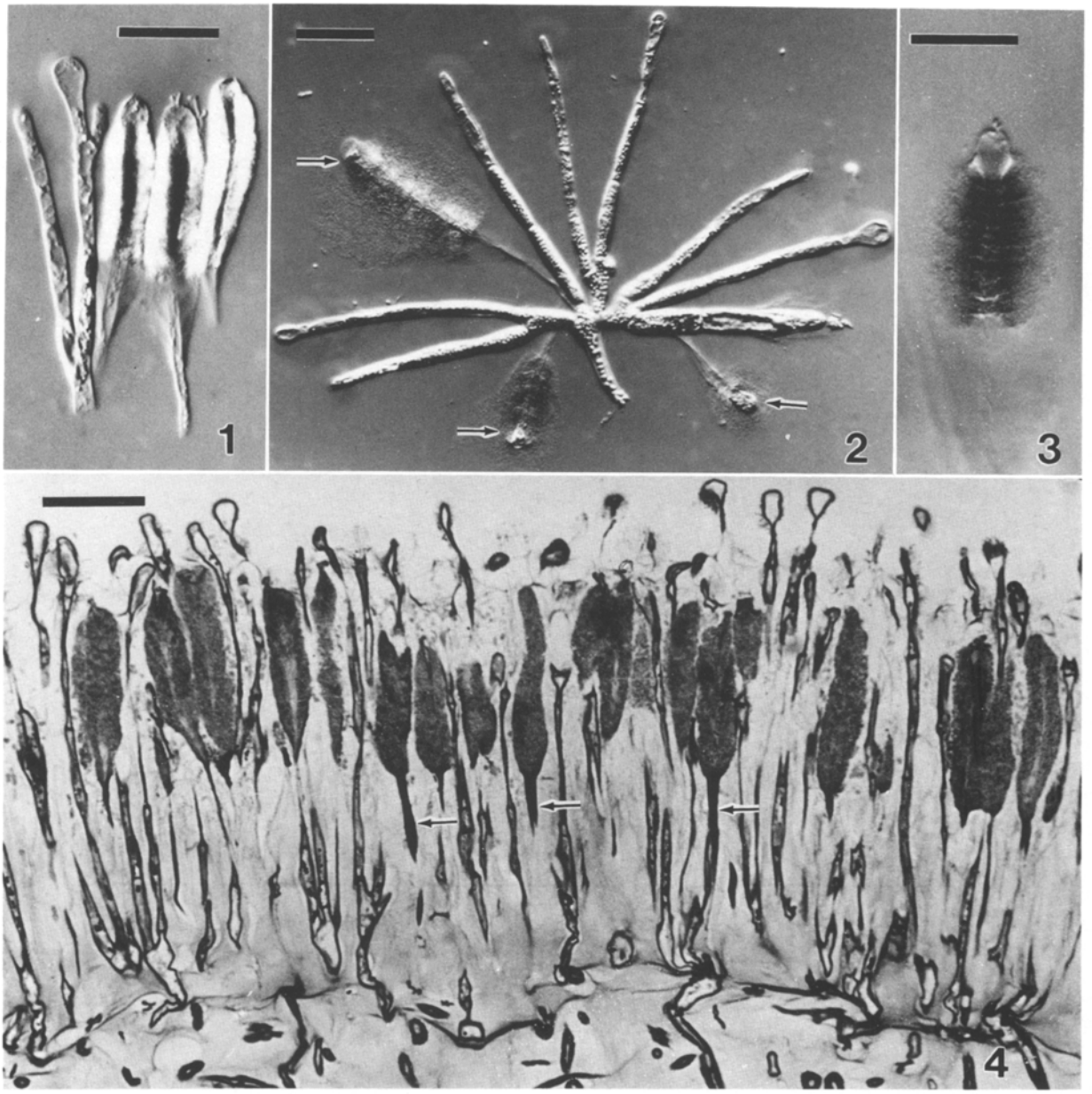

Figs. 1–4. Light micrographs of calciferous cells. Bars: 20 μm

Fig. 1. Scrapings from living thallus, in seawater. Mineralized portion of calciferous cells is birefringent, DIC

Fig. 2. Cortical fascicle with several assimilatory filaments. Calciferous cells (arrows) have lost birefringence and integrity of demineralized matrices. Glutaraldehyde, cacodylate buffer, pH 6.5, DIC

Fig. 3. Whorled appearance of decalcified organic matrix. Phosphate buffer, pH 7.2, DIC

Fig. 4. Semi-thick resin section. PAS stains stalks (arrows) and distal mineralization matrix of calciferous cells. Brightfield

---

Figs. 5–8. SEM

Fig. 5. Longitudinal fracture through several calciferous cells. Cell lumens (arrows) appear as median grooves. Bar: 5 μm

Fig. 6. Paradermal fracture of cortex showing transversely cleaved calciferous cells. In most calciferous cells, both walls and lumens (arrows) are flattened. Bar: 5 μm

Fig. 7. Crystalline nature of $CaCO_3$ granules is shown by plane surfaces. Bar: 0.2 μm

Fig. 8. Crystals were removed by mild acid treatment, leaving a collapsed organic matrix. Bar: 1 μm

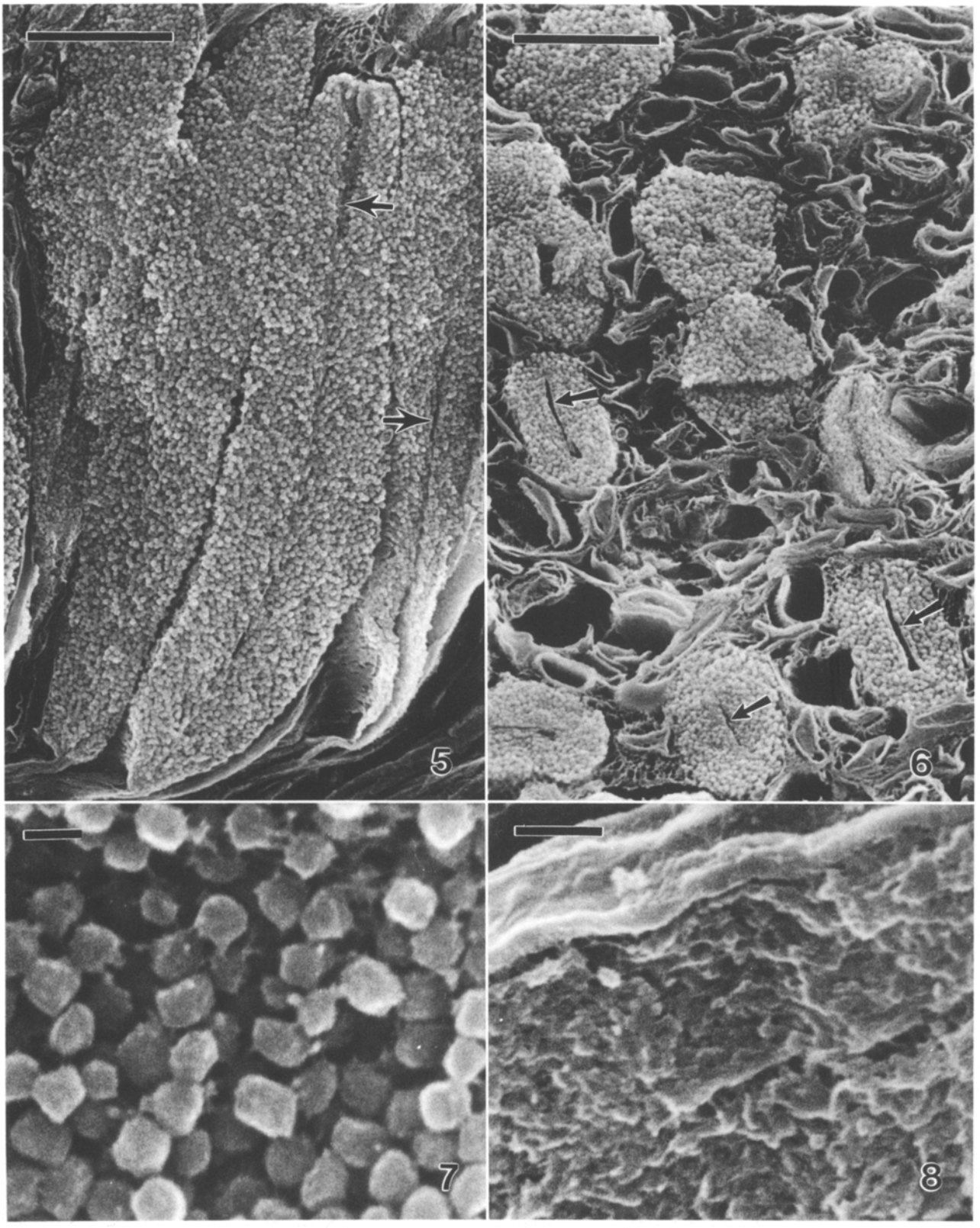
5
6
7
8

mineral deposits were 0.1–0.2 µm thick and were not stained. For routine ultrastructural examination, 60–90 nm thick sections were stained in 2% uranyl acetate followed by Reynolds' lead citrate.

Energy dispersive X-ray microanalysis was performed using a PGT System 4 interfaced with a Hitachi H-7000 TEM. Spectra were collected from unstained sections, ca. 0.2 µm thick, for 100 sec at 75 kV with the microscope in scanning-transmission mode. Spectra were collected from crystals, from the walls immediately adjacent to the crystals, and from areas that included both crystals and cell walls.

Electron diffraction was performed on the same microscope in selective area mode, using silver sections and an acceleration potential of 125 kV. Single crystals with rhombohedral morphology were selected for analysis. A gold standard for calibration of the camera constant was photographed separately, or a sputter coater was used to apply gold directly to sections of the embedded specimen.

Results

Calciferous cells were easily recognized by their mineral deposits, club-like morphology, and length, up to 75 µm (Figs. 1 and 2). They were borne on the same cells that supported assimilatory filaments and were almost as long as entire assimilatory filaments of 4–6 cells. The distal one-half to two-thirds of each mineralized cell was highly refractile under DIC optics (Fig. 1), producing an image of bright edges and a dark midline.

The $CaCO_3$ deposits were embedded in a thick matrix of wall material (Figs. 2–4), but some of the same solutions that removed $CaCO_3$ also extracted the associated organic matrix. Unfixed calciferous cells exposed to 1.0 N HCl lost their distal thickening entirely; the simultaneous loss of mineralization and wall left no evidence of the existence of the latter. Calcium carbonate deposits and most of the wall matrix were lost in TEM and SEM preparations that employed cacodylate buffer at pH 7.2. Fresh specimens in this buffer eventually lost birefringence, but the organic matrix persisted longer, sometimes having a whorled appearance (Fig. 3). Calcium carbonate and its organic matrix were better preserved in phosphate buffer at pH 7.6.

The presence of an organic matrix associated with biomineralization was demonstrated conclusively by PAS, a stain for neutral carbohydrates. The complete form of the mineralized cell wall was produced when imaging only the carbohydrates (Fig. 4). The wall of the stalk-like portion was more densely stained by PAS than was the thicker calcified matrix (Fig. 4), presumably due to the portion of matrix volume occupied by $CaCO_3$, which is PAS-negative.

SEM examination showed the $CaCO_3$ deposits to be composed of numerous individual grains, 150–200 nm in diameter. The grains appeared spherical at low magnification (Figs. 5 and 6), but angular outlines of some grains were seen at high magnification (Fig. 7). Among the grains were fine fibrils, presumably remnants of the organic matrix. Cells exposed briefly to dilute hydrochloric acid in ethanol during specimen dehydration lost the $CaCO_3$ grains, but matrix, though somewhat collapsed, was visible (Fig. 8).

Specimens prepared for TEM using a fixative in phosphate buffer, pH 7.6, retained $CaCO_3$ crystals. The crystals appeared in sections as electron-dense grains, rhombohedral to roughly circular in outline (Figs. 9 and 10). The grains were not infiltrated by the embedding resin, so tears in the resin and loss of grains were common (Fig. 9). Calcium carbonate grains were entirely removed by staining sections with uranyl acetate or lead citrate (Fig. 11). It was not determined whether chemical dissolution or mechanical stress from staining and washing of sections was responsible for extraction of mineral deposits.

Staining of sections allowed visualization of the fibrillar component of the mineralization matrix. Location of $CaCO_3$ grains was apparent as holes in the resin (Figs. 11–14). Thick, electron-dense fibrils formed a reticulum. Holes left by lost $CaCO_3$ particles were lined by fibrils and were relatively evenly distributed within the reticulum (Fig. 11).

The most puzzling feature of the calciferous cells was the condition of the cellular contents. In longitudinally fractured cells viewed with SEM, the cell lumen appeared as little more than a crease in the middle of the thick walls (Fig. 5). The cells were better defined in paradermal fractures, but the lumen appeared flattened, with little space between opposing cell walls (Fig. 6). The flattened cell shape may be an artifact resulting from the plasticity of the wall composed of individual $CaCO_3$ grains.

In TEM preparations, the contents of the calciferous cells were electron-dense and amorphous (Figs. 12–14), when they could be detected at all. Areas of differing density were found, but organelles could not be identified with confidence. The cellular contents appeared to be in a state of degeneration, not artifactual alteration. Some cells had a bulbous tip that was covered by a relatively thin part of the cell wall. TEM examination confirmed that the highly elongated calcified structures were, in fact, individual cells, each with a normal pit plug at its base. Despite the degenerate appearance of the calciferous cells, no evidence was found that pit plugs at the base of these cells were sealed off by either the calciferous cell or its subtending cell.

X-ray spectra were collected from 0.2 µm thick sections of embedded specimens. Individual crystals (Fig. 15),

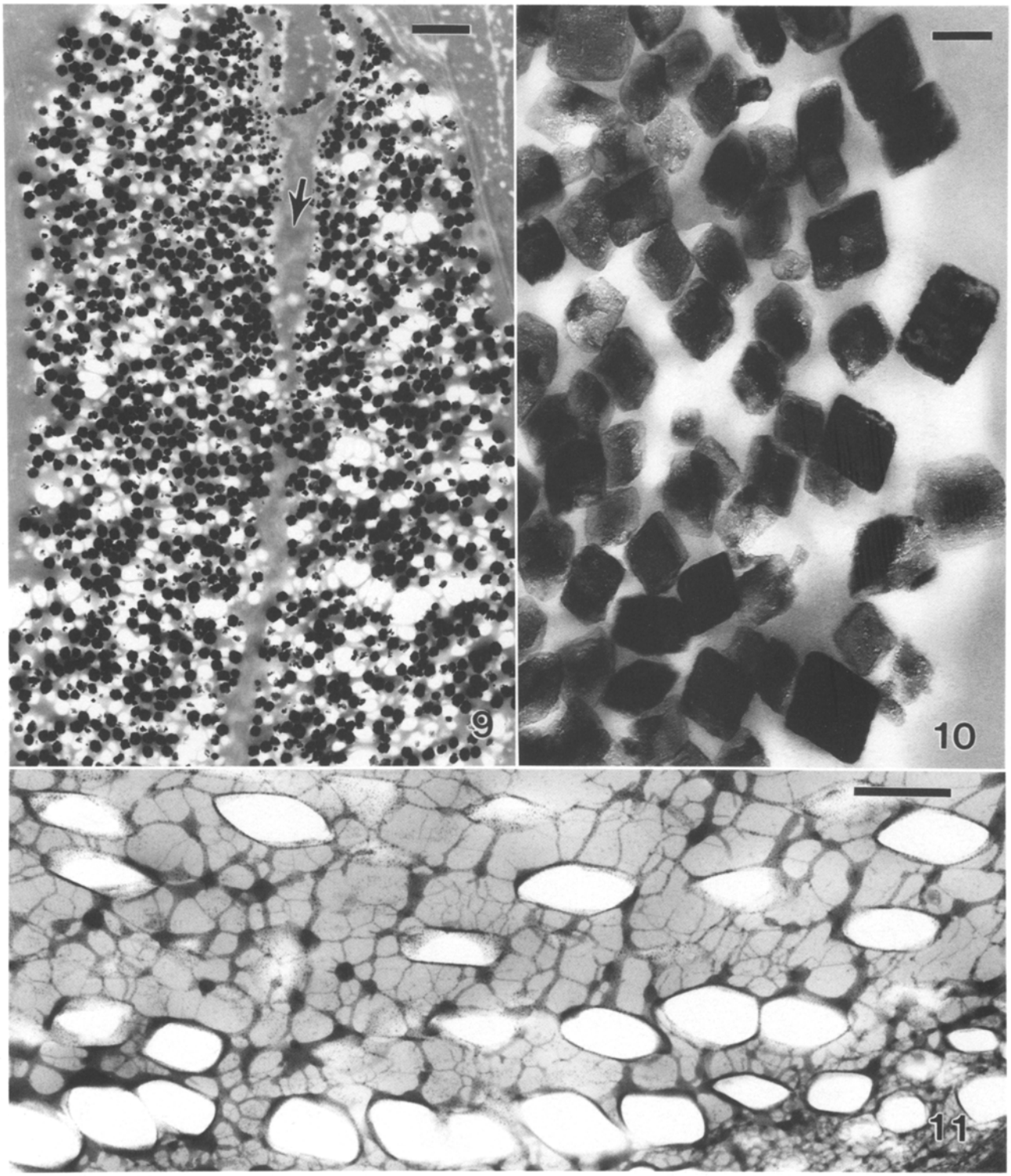

Figs. 9–11. TEM. Sections 1.5 to 2.0 μm thick

Fig. 9. Unstained section. $CaCO_3$ crystals are electron-dense. Note cell lumen (arrow). Bar: 1 μm

Fig. 10. Unstained section. Some particles are clearly rhombohedral. Bar: 0.1 μm

Fig. 11. Uranyl acetate, lead citrate staining removed $CaCO_3$, leaving holes (electron-transparent areas) in section. Organic matrix has fibrillar component that forms a reticulum in which mineral deposits were embedded. Bar: 0.25 μm

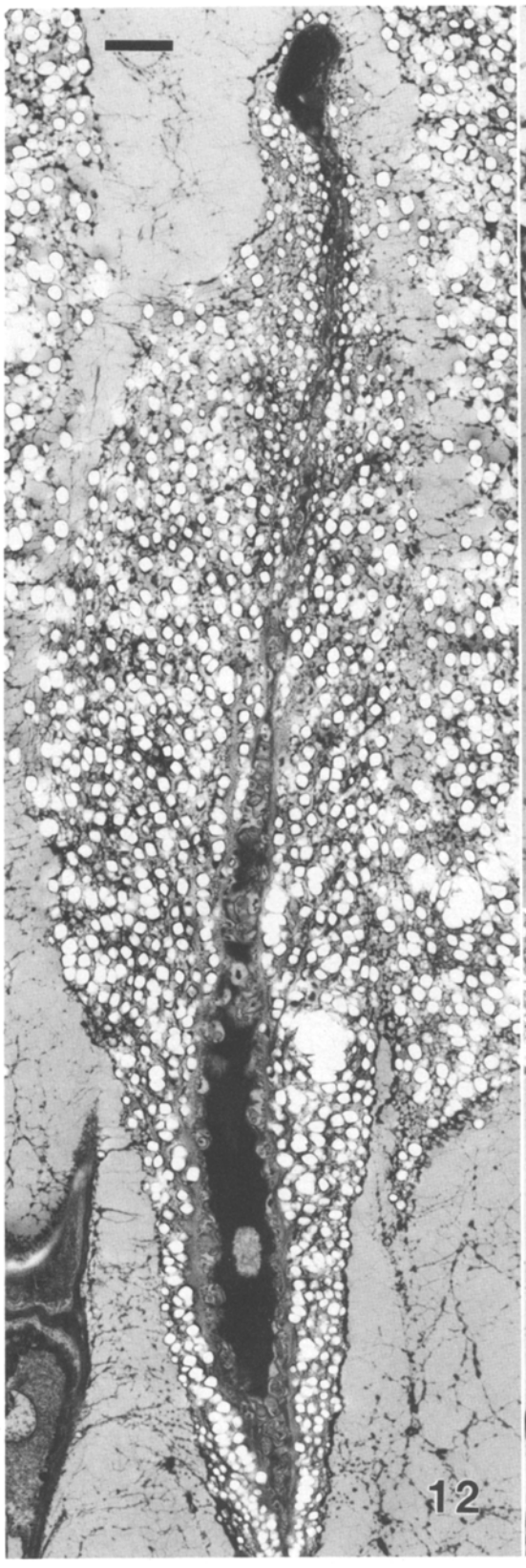
12

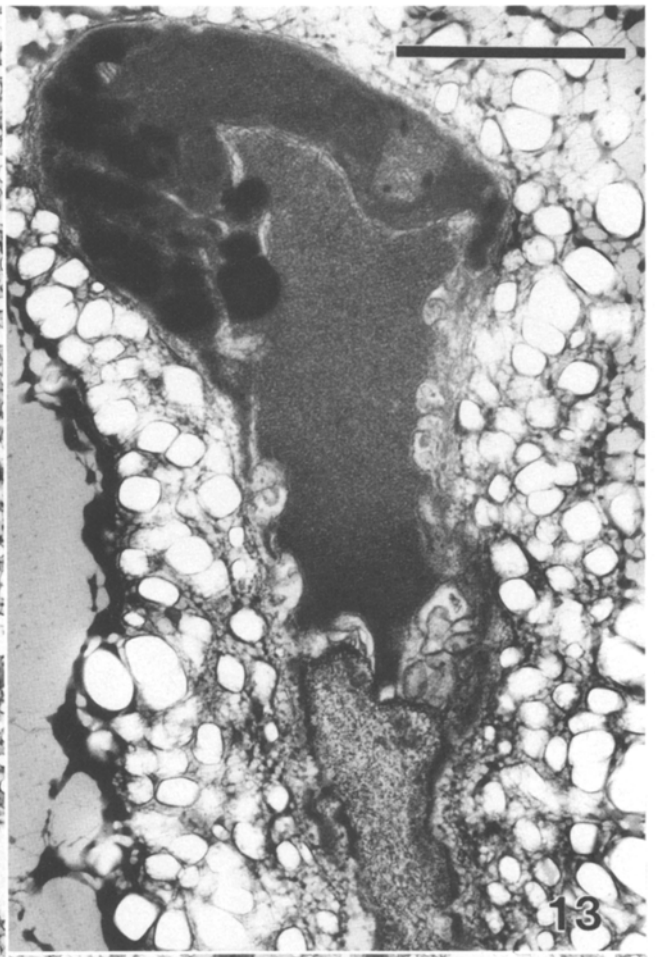
13

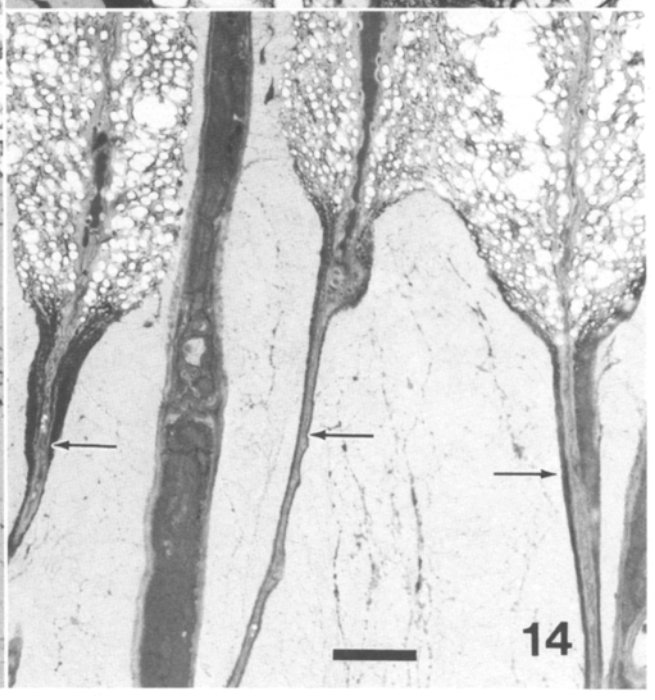
14

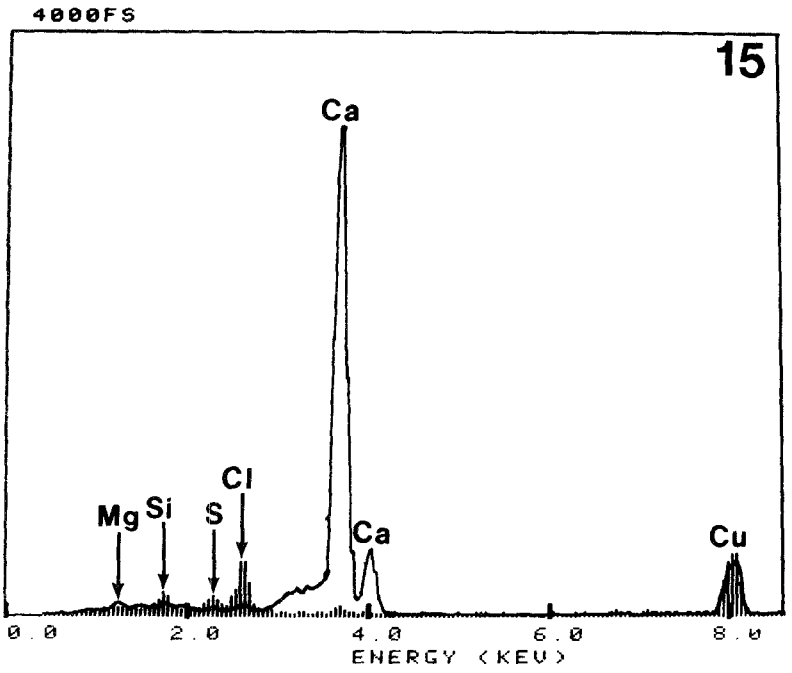

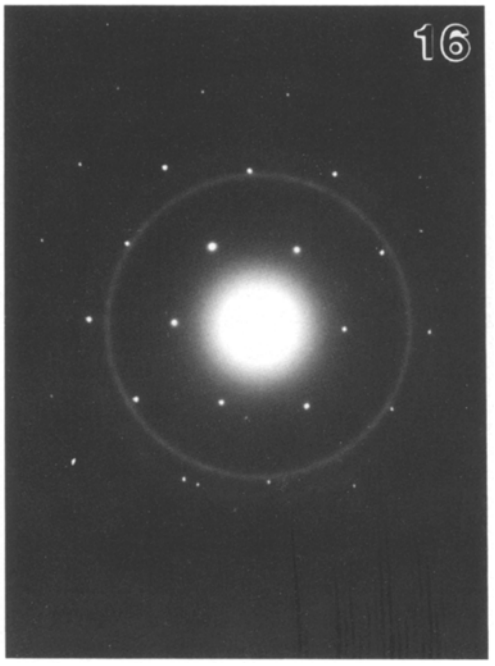

Fig. 15. Energy dispersive X-ray spectrum of individual $CaCO_3$ crystal (solid line) superimposed with spectrum collected from matrix immediately adjacent to crystal (vertical bars)

Fig. 16. Electron diffraction pattern generated from selected area analysis of a single $CaCO_3$ crystal. Rings are from gold sputtered onto the section to serve as a standard for calibration of camera constant. The most prominent ring represents the hkl(111) of gold

organic matrix immediately adjacent to crystals (Fig. 15), and large areas containing many crystals and the matrix surrounding them were analyzed. All spectra showed a small copper K_α peak due to the copper support grid. When electron-dense crystals were analyzed, the K_α and K_β of calcium were the only peaks, other than copper, that were conspicuously above background (Fig. 15). The X-ray detector had a beryllium window, so light elements, including carbon and oxygen in the carbonate, were not detectable. Spectra collected from the organic matrix had a small chlorine peak not seen in spectra gathered from crystals (Fig. 15), presumably due to the abundance of chlorine in the embedding resin; the resin was able to infiltrate cell walls but not mineral deposits. Sulfated wall carbohydrates probably were responsible for a small sulfur peak that was found in spectra of the matrix but not in spectra of crystals. A very small magnesium peak sometimes was detectable in crystals (Fig. 15).

Despite the characteristic calcitic morphology (Fig. 10) of crystals chosen for analysis and the elemental purity of the mineral deposits, as indicated by X-ray microanalysis (Fig. 15), electron diffraction patterns (Fig. 16) showed variations from the d-spacings appropriate for pure calcite.

Discussion

Calcification in *Rhodogorgon* has the following features: the mineral deposits occur as aggregations of discrete particles; calcification is limited to a particular cell type mixed in with uncalcified cells; calcification occurs only within the carbohydrate matrix surrounding part of the calciferous cells; the contents of the calciferous cells are either degenerate or exceptionally sensitive to fixation; and the mineral form of the $CaCO_3$ deposits is calcite. This combination of features is unique and provides a valuable perspective on the cal-

Figs. 12–14. TEM, longitudinal views of stained calciferous cells

Fig. 12. Contents of calciferous cell are dense and disorganized; organelles can not be identified with certainty. Bar: 1 μm

Fig. 13. Apical end of a calciferous cell containing distinct but unrecognizable structures. Bar: 1 μm

Fig. 14. Thick-walled, calciferous part of cell is borne on slender, uncalcified stalk (arrows). Bar: 2 μm

cification process in other algae, especially the calcite-depositing Corallinales.

The question of why some algae and aquatic plants calcify their cell walls and others do not, does not have a simple answer (Borowitzka 1982a, 1984). In *Rhodogorgon*, the question is even more intriguing; why do some cells calcify when adjacent cells do not. One striking difference between calcified and uncalcified cells is the nature of the cell walls. A thick, PAS-positive wall layer, containing a network of fibrillar material is uniquely associated with calcification. Not only is calcification restricted to cells with this type of wall; it is restricted to the distal portion of the calciferous cells, where the thick wall is located. The stalks of these cells are thin-walled and uncalcified. Clearly, the calcification process in *Rhodogorgon*, as in the Corallinales (Borowitzka 1982a, b; Cabioch and Giraud 1986; Pentecost 1980), involves a carbohydrate matrix. The precise association of organic matrix and calcification in *Rhodogorgon* could provide a unique experimental system for the study of matrix calcification.

The morphology of $CaCO_3$ crystals in *Rhodogorgon* differs from that found in Corallinales and in other algae, as well (Borowitzka et al. 1974). Giraud and Cabioch (1979) described the $CaCO_3$ crystals first deposited in growing regions of corallinalean species as being needle-like and tangentially oriented to the cell surface. Subsequent deposition saturates the wall with thicker, but still elongate crystals whose long axis is oriented perpendicular to the cell surface (Borowitzka et al. 1974, Borowitzka 1982a, Cabioch and Giraud 1986, Giraud and Cabioch 1979). Elongate crystals were not observed in *Rhodogorgon*. The smallest crystals were often the most geometrically precise rhombohedral particles. Other particles were less angular, but they were not elongated, never fused, and lacked the typical crystal orientation found in the Corallinales. The size of *Rhodogorgon* crystals was relatively uniform, 150–200 nm in longest dimension. How mineralization in *Rhodogorgon* gives rise to unfused, uniform crystals is yet another problem to be addressed.

The calcification matrix in *Rhodogorgon* consists of a reticulum of dense fibrils. Calcareous crystals appear to be surrounded by a coating of organic material and to occupy spaces within the reticulum. This might be viewed as evidence in support of the compartment hypothesis (Pentecost 1980) and perhaps an explanation for the relatively uniform size and lack of fusion of crystals. However, caution is required in drawing conclusions about the possibility of an organic template for crystal growth. Crystal growth within a completely homogeneous matrix could cause deformation of the matrix, redistributing the wall material to conform to the shape of the growing crystals. Rather than the matrix acting as a template for the crystals, the crystals might mold the matrix constituents to their own morphology. To some extent, matrix fibrils in *Rhodogorgon* may be gathered and compressed by crystal growth, but the existence of a reticulum apart from the crystals is clear.

The calcification matrix sometimes had the appearance of a whorled substructure in light microscopic images (Fig. 3) (Pueschel et al. 1992: Fig. 2), but SEM and TEM images of the calciferous cells did not show this feature so clearly.

That calcification is specific to particular cells implies distinctive features of those cells. In most models of plant calcification, photosynthesis is necessary for $CaCO_3$ precipitation (Borowitzka 1982a, 1984; Digby 1977; Pentecost 1985). In the simplest model, photosynthetic utilization of carbon dioxide increases the alkalinity of the external cellular environment, thus favoring carbonate, which precipitates if calcium is present (Borowitzka 1982a, 1984). Given there is little or no photosynthetic apparatus evident in calciferous cells of *Rhodogorgon*, photosynthetic activity of these cells could not drive biomineralization. Calcification by nonpigmented cells in corallinalean algae is believed to be supported by translocation (La Velle 1979, Pearse 1972). Pit plugs between calcified cells and subtending cells have normal structure and are not sealed off by wall material, so the possibility of translocation to calcifying cells of *Rhodogorgon* cannot be discounted. However, if photosynthetic activity of assimilatory cortical cells supports calcification, why are these photosynthetic cells not calcified? In the absence of photosynthetic activity of the calcified cells, metabolically-driven models of calcification would require all the following features: translocation of a diffusible substance along a gradient towards the calcifying cells, viability of calcifying cells, and restriction of efflux of the ionic species directly involved in calcification to calcifying cells. These requirements constrain some theories of algal calcification. The complexities of physiologically-driven calcification of specialized cells contrasts strongly with the simple observation that calcified and uncalcified cells differ in the nature of their cell coverings. The thick organic matrix of the calcified cells must play a significant role in nucleating $CaCO_3$ crystals.

Halimeda and other calcified, siphonous green algae are able to generate an alkaline environment in which

carbonate precipitation can occur by having an anatomy that restricts diffusion into and out of the cortical intercellular space (Borowitzka 1982 a, Borowitzka and Larkum 1976). From SEM images of the thallus surface of *Rhodogorgon* (Pueschel et al. 1992), it is clear that calcified cells are just beneath the cortical surface, not buried deep in the cortex, and there is no layer of laterally contiguous apical cells forming a barrier to diffusion. As in the Corallinales, cell walls in *Rhodogorgon* are thick and relatively open to the environment. This condition makes it more difficult to explain how photosynthetically incompetent cells are able to calcify.

The function of calcification in *Rhodogorgon* is obscure (Norris and Bucher 1989). Calcification involves only specialized cells and may not be abundant enough to provide mechanical strength, deter herbivores, or significantly reduce illumination, functions commonly ascribed to calcification (Pentecost 1980). But if $CaCO_3$ is viewed as an undesirable physiological by-product, then cells specialized to nucleate $CaCO_3$ precipitation could provide a means of controlling $CaCO_3$ concentration with minimal adverse effect.

Differences in the mineral forms of $CaCO_3$ deposited by red algae show some systematic correlations. All Corallinales deposit calcite, whereas mineralizing Nemaliales and *Peyssonnelia* (Gigartinales) deposit aragonite (Borowitzka et al. 1974). Calcite deposition in *Rhodogorgon* might be viewed as suggesting an affinity with the Corallinales, but calcite formation by members of the Batrachospermales has been reported (Probeguin 1954). Ultrastructural features of pit plugs in *Rhodogorgon* (Pueschel et al. 1992) are consistent with affinities to either of these two orders. Interpretation of possible systematic affinities based on $CaCO_3$ crystal forms are not entirely straightforward. Thermodynamics favor the formation of calcite, but in the presence of cations, aragonite is deposited more readily (Borowitzka 1982 a). As a result, calcite deposition is favored in freshwater and aragonite is favored in marine waters. An organic matrix is considered crucial for the deposition of calcite in marine waters, but unnecessary in freshwater. The context in which calcification occurs, not just the mineral form, must be considered. Both freshwater and marine species may deposit calcite, but Corallinales deposit in an organic matrix and Batrachospermales do not (Pobeguin 1954). It is clear that *Rhodogorgon* deposits calcite in an organic matrix; however, all other aspects of calcification in the Corallinales and *Rhodogorgon* are different and offer little support for homology.

Although $CaCO_3$ is the predominant mineral deposit of red algae, other inorganic deposits are formed. In an X-ray diffraction study of fifteen samples representing several genera of Corallinales, Chave (1954) found that magnesium carbonate made up 7–29% of the total mineral deposits. Magnesium hydroxide and strontium carbonate have also been reported in smaller amounts (Borowitzka et al. 1974). Energy dispersive X-ray microanalysis of individual crystals in *Rhodogorgon* showed them to be almost entirely calcium compounds, with only a trace of magnesium. Rates of magnesium deposition in corallines varies with season (Chave and Wheeler 1965) and growth rate (Moberly 1968). Flajs (1977) demonstrated that wall layers of some corallines differed markedly in their magnesium content. Our X-ray microanalysis addresses only the purity of individual grains and may not be representative of the mineralogical composition of the entire thallus at all seasons.

Electron diffraction results suggest that there are impurities in the calcite crystals. The small amounts of magnesium detected by elemental analysis may have been responsible, or perhaps components of the organic matrix were incorporated into the crystals. Glycoprotein components in sea urchin spines change the fracture planes from crystalline cleavage expected for pure calcite to conchoidal fractures, typical of amorphous materials (Berman et al. 1990). The crystals in *Rhodogorgon* were too small to be split by the cleavage plane during cryofracturing for SEM, so observations of crystal fracture faces were not possible.

The remarkable features of calcification in *Rhodogorgon*, especially its restriction to a specialized cell type, the calciferous cell, make this alga an excellent subject for detailed study of the calcification process.

Acknowledgements

The authors thank James Norris and Katina Bucher, Smithsonian Institution, for bringing this alga to our attention, for their collaboration with field work at Carrie Bow Cay, Belize, and for their comments on the manuscript. Principal financial support was provided by NSF grant BSR 88-1802 to CMP. This study represents contribution #323 of the Smithsonian Institution's Caribbean Coral Reef Program (CCRE), partially supported by the Exxon Corporation. Field study in Belize was made possible by CCRE support.

References

Berman A, Addadi L, Kvick A, Leiserowitz L, Nelson M, Weiner S (1990) Intercalation of sea urchin proteins in calcite: study of a crystalline composite material. Science 250: 664–667

Borowitzka MA (1982 a) Mechanisms in algal calcification. Prog Phycol Res 1: 137–177

Borowitzka MA (1982 b) Morphological and cytological aspects of algal calcification. Int Rev Cytol 74: 127–162

– (1984) Calcification in aquatic plants. Plant Cell Environ 7: 457–466

– Larkum AWD (1976) Calcification in the green alga *Halimeda* III. The sources of inorganic carbon for photosynthesis and a model of the mechanism of calcification. J Exp Bot 27: 879–893

– – Nockolds CE (1974) A scanning electron microscope study of the structure and organization of the calcium carbonate deposits of algae. Phycologia 13: 195–203

Cabioch J, Giraud G (1986) Structural aspects of biomineralization in the coralline algae (calcified Rhodophyceae). In: Leadbeater BSC, Reading R (eds) Biomineralization in lower plants and animals. Clarendon, Oxford, pp 141–156

Chave KE (1954) Aspects of the biogeochemistry of magnesium 1. Calcareous marine organisms. J Geol 62: 266–283

– Wheeler BD Jr (1965) Mineralogic changes during growth in the red alga, *Clathromorphum compactum*. Science 147: 621

Digby PSB (1977) Photosynthesis and respiration in the coralline algae, *Clathromorphum circumscriptum* and *Corallina officinalis* and the metabolic basis of calcification. J Mar Biol Assoc UK 57: 1111–1124

Flajs G (1977) Die Ultrastrukturen des Kalkalgenskeletts. Palaeontographica [B] 160: 69–128

Giraud G, Cabioch J (1979) Ultrastructure and elaboration of calcified cell-walls in the coralline algae (Rhodophyta, Cryptonemiales). Biol Cell 36: 81–86

La Velle JM (1979) Translocation in *Calliarthron tuberculosum* and its role in the light-enhancement of calcification. Mar Biol 55: 37–44

Moberly R Jr (1968) Composition of magnesian calcites of algae and pelecypods by electron microprobe analysis. Sedimentology 11: 61–82

Nation JL (1983) A new method using hexamethyldisilazane for preparation of soft insect tissues for scanning electron microscopy. Stain Technol 58: 347–351

Norris JN, Bucher KE (1989) *Rhodogorgon*, an anamolous new red algal genus from the Caribbean Sea. Proc Biol Soc Wash 102: 1050–1066

Pearse VB (1972) Radioisotopic study of calcification in the articulated coralline alga *Bossiella orbigniana*. J Phycol 8: 88–97

Pentecost A (1980) Calcification in plants. Int Rev Cytol 62: 1–27

– (1985) Photosynthetic plants as intermediary agents between environmental HCO_3^- and carbonate deposition. In: Lucas WJ, Berry JA (eds) Inorganic carbon uptake by aquatic photosynthetic organisms. American Society of Plant Physiologists, Rockville, pp 459–480

Pobeguin T (1954) Contribution a l'étude des carbonates de calcium précipitation du calcaire par les végétaux comparaison avec le monde animal. Ann Sci Nat Bot 11: 29–109

Pueschel CM, Trick HN, Norris JN (1992) Fine structure of the phylogenetically important marine alga *Rhodogorgon carriebowensis* (Rhodophyta, Batrachospermales?). Protoplasma 166: 78–88

Silva PC, Johansen HW (1986) A reappraisal of the order Corallinales (Rhodophyceae). Br Phycol J 21: 245–254